DEUTSCHES ELEKTRONEN-SYNCHROTRON DESY

DESY 82-081
December 1982



# A CALCULATION OF THE ELECTROMAGNETIC VACUUM POLARIZATION IN LATTICE QCD

by

A. Ali

*Deutsches Elektronen-Synchrotron DESY, Hamburg*

I. Montvay

*II. Institut für Theoretische Physik der Universität Hamburg*

ISSN 0418-9833

NOTKESTRASSE 85 · 2 HAMBURG 52

To be sure that your preprints are promptly included in the
HIGH ENERGY PHYSICS INDEX ,
send them to the following address ( if possible by air mail ) :

DESY
Bibliothek
Notkestrasse 85
2 Hamburg 52
Germany

DESY 82-081
December 1982

ISSN 0418-9833

# A Calculation of the Electromagnetic Vacuum Polarization in Lattice QCD

A. Ali

Deutsches Elektronen-Synchrotron DESY

and

I. Montvay *

II. Institut für Theoretische Physik der Universität Hamburg

Abstract

We present a calculation of the electromagnetic current vacuum polarization in the framework of lattice QCD. A 16th order hopping-parameter expansion of $\langle J_\mu^{em} J_\mu^{em} \rangle_0$ is reported on an $8^4$ lattice. It gives a reasonable description of the mass $m_{J/\psi}$ and the electromagnetic current-vector meson coupling constant $f_{J/\psi}$, in the vector meson dominance approximation.

* Supported by the Bundesministerium für Forschung und Technologie, Federal Republic of Germany.



## 1. Introduction

Lattice gauge theories provide a framework to study non-perturbative aspects of strong interactions [1,2,3]. These methods have been used in conjunction with Monte Carlo techniques to calculate the meson-, baryon-, and the glueball mass spectra with encouraging results.

Electromagnetic and weak currents also provide a lot of information about strong interactions via their couplings to hadrons. Therefore, there is a great theoretical interest to calculate these current amplitudes from first principles in the theory of Quantum Chromodynamics, QCD. Recent attempts in this direction have given promising results for the baryon magnetic moments [4,5], and the coupling constant ratio $g_A/g_V$ [6]. The earlier calculations of the vacuum polarization amplitudes based on the Monte Carlo techniques [7,8] have, however, yielded results which are not in quantitative agreement with the data. These latter calculations were done using a small size lattice and the currents were defined at the same space-time point ("naive currents"), which suffer from incalculable renormalization effects.

In this note we reinvestigate the problem of the electromagnetic vacuum polarization by employing a bigger lattice ($8^4$), and defining a point-split current operator which is conserved on the lattice. The use of conserved vector current eliminates at least one of the uncertainties in the calculation, namely the effect of the (finite) unknown normalization constant. Whether the remaining finite lattice spacing effects depending on $a/\xi$ ($a$ = lattice spacing, $\xi$ = correlation length) and the finite lattice size effects depending on $\xi/L$ ($L$ = physical size of the lattice) allow us to reach conclusions about the continuum vacuum polarization amplitude remain to be investigated. Our conclusion

is that we are able to calculate the charm quark vector current amplitude satisfactorily on an $8^4$ lattice. However, a larger lattice is needed to reliably determine the properties of the systems other than charm.

## 2. Method

We start by defining the electromagnetic vacuum polarization amplitude of hadrons as

$$A_{\mu\nu}(x) \equiv \langle 0 | T \{ \mathcal{J}_\mu^{em}(x) \mathcal{J}_\nu^{em}(0) \} | 0 \rangle , \qquad (1)$$

where the electromagnetic current of hadrons $J_\mu^{em}$ is built from the vector current $V_q$ of the quarks with flavours $q$ = u,d,s,c,... in the usual way

$$\mathcal{J}_\mu^{em} = \frac{2}{3} V_\mu^u - \frac{1}{3} V_\mu^d + \frac{2}{3} V_\mu^c - \frac{1}{3} V_\mu^s + \cdots . \qquad (2)$$

The "naive" definition of the vector current would be $V_\mu(x) = \text{const.}\ \bar{\psi}_x \gamma_\mu \psi_x$. This, however, as remarked above contains an unknown, coupling constant dependent (finite) normalization factor, which is difficult to determine in the non-perturbative regime. Therefore, we use the conserved ("point-split") vector current as introduced on the lattice by Karsten and Smit [9]:

$$V_{x,\mu} \equiv K a^{-3} \{ \bar{\psi}_{x+\hat{\mu}} U[x+\hat{\mu}, x] (1+\gamma_\mu) \psi_x - \bar{\psi}_x U[x, x+\hat{\mu}] (1-\gamma_\mu) \psi_{x+\hat{\mu}} \} . \qquad (3)$$

Here $U[x+\hat{\mu}, x]$ denotes the gauge field variable belonging to the link $[x+\hat{\mu}, x]$, $\gamma_\mu$ is the (euclidean, hermitian) Dirac matrix acting on



the quark fields $\psi_x$, $\bar{\psi}_x$, and the Wilson hopping parameter K is connected to the bare quark mass m via the relation

$$K = (8 + 2am)^{-1}$$

In the case of the Wilson-action for fermions (which we use in the present paper) the equations of motion on the lattice imply the current conservation equation

$$\sum_{\mu=1}^{4} \nabla_\mu V_{x-\hat{\mu},\mu} \equiv \sum_\mu a^{-1} \left[ V_{x,\mu} - V_{x-\hat{\mu},\mu} \right] = 0 . \qquad (4)$$

The advantage of the point-split current is that it is correctly normalized also at finite lattice spacing a, where the numerical calculations are done. The disadvantage is, of course, the more complicated form making the numerical calculations more difficult.

In our lattice Monte Carlo calculations we consider the "time slices" of the space-like components of the vacuum polarization amplitude

$$T_{rs}(x_4) = \int d^3x \, A_{rs}(\vec{x}, x_4) \qquad (r,s = 1,2,3) \qquad (5)$$

or its Fourier-transform

$$\tilde{T}_{rs}(p_4) = \int dx_4 \, e^{-i p_4 x_4} T_{rs}(x_4) . \qquad (6)$$

The integration over the space coordinates projects out the zero three-momentum intermediate states, therefore the Källen-Lehmann representation of $T_{rs}(x_4)$ and $\tilde{T}_{rs}(p_4)$ is, respectively,

$$T_{rs}(x_4) = \delta_{rs} \int_0^\infty dm^2 \, \rho(m^2) \, \frac{e^{-x_4 m}}{2m} \quad ; \tag{7}$$

$$\tilde{T}_{rs}(p_4) = \delta_{rs} \int_0^\infty dm^2 \, \rho(m^2) \left(p_4^2 + m^2\right)^{-1} \quad . \tag{8}$$

We remark that one could make a direct comparison of the lattice QCD calculation of the vacuum polarization density, $\tilde{T}_{rs}(p_4)$, with the experimental data in $e^+e^-$ annihilation. Defining $\tilde{T}_{rs}(p_4) \equiv \delta_{rs} \, \pi(p_4^2) p_4^2$, one could write a dispersion relation to relate $\pi(p_4^2)$, calculated at space-like momenta $p_4^2$, to the hadronic cross-section ratio $R \equiv \sigma(e^+e^- \to \text{hadrons}) / \sigma(e^+e^- \to \mu^+\mu^-)$ measured at time-like momenta. In the form of once subtracted relation one has, for example, for the isospin -1 current of $J_\mu^{em}$

$$\pi^{I=1}(-s_1) - \pi^{I=1}(-s_2) = \frac{(s_2 - s_1)}{12\pi^4} \int_{4m_\pi^2}^\infty ds \, \frac{R^{I=1}(s)}{(s+s_1)(s+s_2)} \quad , \tag{9}$$

where

$$(p_4^2)_i = -s_i < 0 \quad (i = 1,2) \, .$$

Experimental data at low s could be combined with the (small) perturbative QCD contribution at large $s$ to evaluate the right hand side. Lattice QCD provides the left hand side.

The present Monte Carlo calculations are limited to moderate values of energy ($p_4^{max.} = \pi/a$). Phenomenology tells us that the vacuum polarization amplitude at these energies are dominated by the appropriate vector-meson poles

$V = \rho, \omega, \phi, J/\psi, \ldots$ . In the pole dominance approximation the spectral function $\rho(m^2)$ is given by



$$\rho(m^2) = \sum_V m_V^4 \, f_V^{-2} \, \delta(m^2 - m_V^2) \quad . \tag{10}$$

Thus, measuring the time slices $T_{rs}(x_4)$ on the lattice one can extract the masses ($m_V$) and the electromagnetic decay constant ($f_V$) of the vector mesons. We shall assume vector meson dominance in the following.

The results presented here are based on our Monte Carlo data on an $8^4$ lattice with SU(3) colour gauge group. The effect of the quark determinant was neglected ("quenched approximation"). We have employed the hopping parameter expansion technique of refs. (10) and (11) to determine the function $T_{rs}(x_4)$:

$$T_{rs}(x_4) = \sum_{l=l_{min}}^\infty K^{2l} \, C_{rs}(l; x_4) \, . \tag{11}$$

Periodic boundary conditions were used both for the gauge fields and the quark fields ("periodic box" case of ref. (11)). The 16th order hopping parameter series was obtained for two values of $\beta = 6g^{-2} = 5.7$ and 6.0. At $\beta = 5.7$ we have calculated the quark propagator on 5 independent gauge field configurations, whereas for $\beta = 6.0$ on 3 configurations. On each gauge field configuration we have chosen 16 initial points for the quark propagation. In order to reduce correlations, the gauge fields were prepared independently from each other iterating on both "hot" and "cold" starts as well as on "mixed" ones (half parallel, half random link variables). At least 300 Metropolis sweeps per configuration were performed with 6 updatings per link.

The results for the 16th order hopping parameter expansion coefficients $c_{11}(l; x_4)$ (for the point-split current components r = s = 1) are collected in table 1 for $\beta = 5.7$ and 6.0. The entries shown are averaged over the negative and positive time direction which should be equal with infinite statistics. The statistical errors are typically a few percent for the lower coefficients and grow up to

about 10 percent in the 16th order. We remark that the statistical errors on the point-split current coefficients $C_{11}(\ell, x_4)$ are at least a factor 2 larger (with comparable statistics) than the corresponding errors on the coefficients of the "naive" current. This presumably stems from the two opposite-sign terms (in Eq. (3)) implying numerical cancellations in the matrix elements. On the other hand, up to the 16th order there is no sign change in the coefficients of the point-split current contrary to the "naive" current.

The amplitudes have to be calculated for different values of the hopping parameter $K = K_u, K_d, K_s, K_c, \ldots$ belonging to different quark flavours. These values are not known a priori and have to be determined for each quark flavour by fixing, for example, the corresponding vector meson mass at a given value of the lattice-spacing a. The flavour structure of the vacuum polarization amplitude corresponding to Eq. (2) is in the isovector (IV) and the isoscalar (IS) channels, respectively:

$$A_{IV}(x)_{\mu\nu} = \frac{1}{2} C_{uu}(x)_{\mu\nu} ,$$

$$A_{IS}(x)_{\mu\nu} = \frac{1}{18} C_{uu}(x)_{\mu\nu} + \frac{1}{9} C_{ss}(x)_{\mu\nu} + \frac{4}{9} C_{cc}(x)_{\mu\nu} + \ldots \quad (12)$$

Here $C_{qq}$ denotes the amplitude for the two vector currents (3) with the same quark flavour q. /F1/

## 3. Analysis and Results

The most direct way is to analyse the function $T_{rs}(x_4)$ evaluated with the help of the entries in tables 1 . In the pole dominance approximation, this amounts to determining the vector meson mass $m_v$, through the exponential



fall-off of the correlation function $T_{rs}(x_4)$; the amplitude $f_v$ is then determined using Eqs. (7) and (10), fixing a. However, this program is difficult to carry out due to our large statistical errors (typically $\pm$ 10 %) on the coefficients with $x_4 = 3$ and 4 and the fact that the apparent radius of convergence of the series $C(\ell, x_4 = 3,4)$ (estimated e.g. by a ratio test) is rather small in the hopping parameter space. So, even if one uses the Padé approximants to analytically continue in the K-space, one needs large extrapolations to reach the physical values of $K_u$, $K_s$ etc. Consequently, the various Padés don't converge to a definite value.

The situation in the p-space is much better, however. The apparent radius of convergence of the hopping parameter series for the Fourier transformed amplitude $\tilde{T}_{rs}(p_4)$ is much larger. Thus, the Padé extrapolation in K is more stable. Therefore, we Fourier-transformed the coefficients in table 1 to the discrete points in the momentum space

$$p_4 = \frac{\pi}{4a} k_4 \qquad (k_4 = B_4, B_4+1, \ldots, B_4+7). \quad (13)$$

These points in the momentum space correspond to the $8^4$ periodic boundary conditions which we use (both for the gauge and quark fields). The integer number $B_4$ specifying the lowest point of the Brillouin-zone is arbitrary. To be definite, we have taken $B_4 = -3$.

From the hopping parameter expansion coefficients in the momentum space we construct the amplitude $\tilde{T}_{11}(p_4)$ and determine its value for the various hopping parameters K by using the Padé approximants. Having the values of the amplitudes $\tilde{T}_{11}(p_4)$ one can determine the position of the pole, $m_v$, and the coupling constant

$f_v$ using Eqs. (8) and (10). The best values are obtained from the amplitudes at the smallest momenta $p_4 = 0$ and $\pi/4$, which are nearest to the pole. However, we have checked that any other combination of the three smallest momenta $(0, \pi/4, \pi/2)$ give only slightly different pole parameters. In the range below $K \simeq 0.10$, the Padé table is rather stable and we obtain practically the same values from all the Padé's, except for a few low order ones. This can be seen in table 2, where we list the various Padés for the quantities $am_v$ and $f_v^{-1}$. Above $K \simeq 0.10$, the Padé table becomes somewhat worse, but a reasonable extrapolation can still be obtained up to about $K \simeq 0.13$ (somewhat better for $\beta = 5.7$ and worse for $\beta = 6.0$, where the radius of convergence of the hopping series is smaller and our statistics poorer).

Another method of extracting $m_v$ and $f_v$ is to Fourier transform the amplitude obtained in the p-space from the Padé analysis back to the coordinate space, and determine the pole characteristics through the large $x_4$ values of the function $T_{11}(x_4)$ so obtained. We remark that the analytic continuations in the momentum- and coordinate space are not equivalent due to the non-linearity of the Padé approximants. We have performed an analysis both for the $\tilde{T}_{11}(p_4)$ and the $T_{11}(x_4)$ amplitudes which give consistent result as shown in Fig. (1). The statistical errors, however, propagate lot more in the x-space in the determination of $m_{J/\psi}$ and $f_{J/\psi}$. In Fig. (2) we compare the results of the p-space analysis for $f_{J/\psi}^{-1}$ and $m_{J/\psi}$ obtained by the "point-split" current (16th order series) and the "naive" current obtained from a 32-order hopping parameter expansion.

Now we come to the results. It can be seen from the figures that our present $8^4$ lattice, and statistics (80 points at $\beta = 5.7$ and 48 at $\beta = 6.0$) are not good



enough to warrant a definitive determination of the properties of the light quark (u,d,s) systems. We recall that our Padé approximant method ceases to be convergent above K = 0.13. Let us therefore concentrate on the $J/\psi$ meson. At $\beta = 5.7$ (Fig. 2), the vector meson mass determined from the naive current ( $\bar{\psi}_x \gamma_\mu \psi_x$ ) and the point-split current is the same within errors, for K in the charm quark region. The value of $f_{J/\psi}^{-1}$ for the two currents is also very similar for $K \lesssim 0.7$. However, in the $K \gtrsim K_c$ regions the two currents lead to different values for $f_{J/\psi}^{-1}$. For the point-split current we get $am_{J/\psi} = 3.1$ at $K = 0.091$, from which we get $a^{-1} = 1000$ MeV. This is consistent with $a^{-1} = (800 \pm 200)$ MeV at $\beta = 5.7$, obtained from the previous Monte Carlo measurements of the string tension in SU(3) [12,13]. The precise values of $K_c$ and $f_{J/\psi}^{-1}$ at $\beta = 5.7$ for $a^{-1} = 1000$ MeV are:

| | | |
|---|---|---|
| Point-split current | $K_c = 0.091$ | $f_{J/\psi}^{-1} = 0.089$ |
| "naive" current | $K_c = 0.089$ | $f_{J/\psi}^{-1} = 0.069$ |

The experimental value $f_{J/\psi}^{-1} = 0.083$ is very well reproduced. At this value of $a^{-1}$ the point-split current gives a better result, whereas the normalization of the "naive" current is off by about 20 %. A better Monte Carlo measurement of $a^{-1}$ from the string tension would provide a better distinction between the two currents. Comparing $\beta = 6.0$ and $\beta = 5.7$ in the $J/\psi$ region we have found little difference in the curves for $f_{J/\psi}^{-1}$. The mass curves are somewhat different. Assuming renormalization group behaviour, $a^{-1} = 1000$ MeV at $\beta = 5.7$ implies $a^{-1} = 1400$ MeV at $\beta = 6.0$. This gives an $f_{J/\psi}^{-1}$ at $\beta = 6.0$, which is a factor $\simeq 2$ larger compared to the value at $\beta = 5.7$. This holds for both the currents. In

other words, there is no evidence of scaling between $\beta$ = 5.7 and 6.0 on the $8^4$ lattice within our statistics.

As far as the light quark (u,d,s) mesons are concerned it is quite clear from Figs. (1) and (2) that $f_V^{-1}$ is too big for V = $\rho$ and $\phi$. We were unable to extrapolate (with Padé approximants) our point-split data to the region $K \cong 0.15 - 0.16$, relevant for the $\rho$ and $\phi$ mesons. The "naive" current data (with smaller errors) can, however, be extrapolated giving $f_\rho^{-1} \cong 0.45$ at $K_u = 0.16$ (where $m_\pi = 0$) and $\beta = 5.7$. This is a factor $\cong 2.4$ larger than the experimental value $f_\rho^{-1} = 0.19$. Similarly, at $\beta = 6.0$, $f_\rho^{-1} \cong 0.56$ at $K = K_u = 0.155$. This a factor $\cong 3.0$ too large compared to $(f_\rho^{-1})_{\text{experiment}}$. The numbers for $f_\rho^{-1}$ are almost identical to the ones obtained in ref. /7,8/ on smaller lattices. In our opinion, the numbers for the light quark system have little to do with the continuum QCD because of the large finite-size effects caused by tunnelling through the periodic lattice potential [11]. These effects are certainly smaller for the heavy quark systems on an $8^4$ lattice, though not entirely negligible.

In conclusion, the magnitude of the charm quark vector current vacuum polarization is reasonably well described on an $8^4$ lattice, somewhat better with the point-split current though the "naive" current prediction is also not too far off the mark. There is, however, no evidence of the renormalization group scaling behaviour between $\beta$ = 5.7 and 6.0. We trust the $\beta$ = 5.7 data more, because the finite volume effects are larger at $\beta$ = 6.0 (more for the point-split current, for obvious reasons). This is so because according to the renormalization group, the linear size of our spatial box is about a factor 1.4 smaller at $\beta$ = 6.0. It is, however, very well possible that the observed non-scaling behaviour is the result of a complicated interplay between the finite lattice spacing- and finite



lattice size effects. We hope to come back to these questions in a future publication.

We would like to thank our colleagues at DESY and the II. Institut für Theoretische Physik at Hamburg for a continuous feedback and lively discussions. In particular we would like to thank F. Gutbrod, P. Hasenfratz, H. Joos, Z. Kunszt, G. Mack, L. McLerran, G. Parisi, K. Symanzik and P. Weisz for useful discussions. We thank T. Walsh for reading the manuscript. The support of the DESY computer center is also thankfully acknowledged.

References

(1) K.G. Wilson, Phys. Rev. D10, 2445 (1974)

(2) M. Creutz, L. Jacobs, C. Rebbi, Phys. Rev. Lett. 42, 1390 (1979); Phys. Rev. D20, 1915 (1979)

(3) M. Creutz, Phys. Rev. Lett. 43, 553 (1979); Phys. Rev. D21, 2308 (1980)

(4) G. Martinelli, G. Parisi, R. Petronzio, F. Rapuano, Phys. Lett. 116B, 434 (1982)

(5) C. Bernard, T. Draper, K. Olynyk, M. Rushton, Phys. Rev. Lett. 49, 1076 (1982)

(6) F. Fucito, G. Parisi, S. Petrarca, Phys. Lett. 115B, 148 (1982)

(7) D. Weingarten, Bloomington preprint IUHET-82 (1982)

(8) H. Hamber, G. Parisi, Brookhaven preprint BNL 31322 (1982)

(9) L.H. Karsten, F. Smit, Nucl. Phys. B183, 103 (1981)

(10) A. Hasenfratz, Z. Kunszt, P. Hasenfratz, C.B. Lang, Phys. Lett. 110B, 289 (1982)

(11) P. Hasenfratz, I. Montvay, Santa Barbara preprint NSF-ITP-82-135 (1982)

(12) M. Creutz, Phys. Rev. Lett. 45, 313 (1980)

(13) E. Pietarinen, Nucl. Phys. B190, 349 (1981)

Footnote

/F1/ Note, that we are neglecting here contributions from disconnected quark diagrams, which are presumably small in the quenched approximation. In fact, for SU(2) colour they would vanish identically, because they are proportional to the imaginary part of colour traces.



Table Captions

Table 1: The current correlation hopping matrix $C_{11}(\ell, x_4)$ in the x-space (defined through Eq. (11)) calculated on an $8^4$ lattice.
a) $\beta = 5.7$
b) $\beta = 6.0$

Table 2: The Padé table for $am_v$ and $f_v^{-1}$ calculated in the p-space at $\beta = 5.7$ on an $8^4$ lattice. The K-values are chosen to approximately correspond to the $J/\psi$ region.

Figure Captions

Fig. 1: A comparison of the p-space and x-space analysis for the inverse lattice spacing $a^{-1}$ and the vector meson coupling constant $f_{J/\psi}^{-1}$ as a function of the hopping parameter K, based on our Monte Carlo data on an $8^4$ lattice at $\beta = 5.7$. The vertical bars denote the uncertainty due to the various Padés in the x-space.

Fig. 2: A comparison of the p-space analysis of the point-split and naive current data for the vector meson mass $am_{J/\psi}$ and the vector coupling constant $f_{J/\psi}^{-1}$.

| $\ell$ \ $x_4$ | 0 | 1 | 2 | 3 | 4 |
|---|---|---|---|---|---|
| 1 | $(1.519 \pm .026)\times10^{3}$ | $(1.102 \pm .048)\times10^{2}$ | 0.0 | 0.0 | 0.0 |
| 2 | $(5.633 \pm .157)\times10^{4}$ | $(5.991 \pm .181)\times10^{3}$ | $(7.436 \pm .037)^{\times10^{1}}$ | 0.0 | 0.0 |
| 3 | $(2.625 \pm .143)\times10^{6}$ | $(7.086 \pm .279)\times10^{5}$ | $(4.808 \pm .185)\times10^{4}$ | $(6.732 \pm .64)\times10^{2}$ | 0.0 |
| 4 | $(1.118 \pm .095)\times10^{8}$ | $(4.081 \pm .221)\times10^{6}$ | $(4.703 \pm .246)\times10^{6}$ | $(1.255 \pm .086)\times10^{5}$ | $(4.747 \pm .172)\times10^{3}$ |
| 5 | $(4.70 \pm .47)\times10^{9}$ | $(2.145 \pm .143)\times10^{9}$ | $(4.539 \pm .229)\times10^{8}$ | $(3.492 \pm .19)\times10^{7}$ | $(1.30 \pm .189)\times10^{6}$ |
| 6 | $(1.933 \pm .182)\times10^{11}$ | $(9.852 \pm .851)\times10^{10}$ | $(2.977 \pm .172)\times10^{10}$ | $(4.203 \pm .218)\times10^{9}$ | $(3.294 \pm .250)\times10^{8}$ |
| 7 | $(7.457 \pm .581)\times10^{12}$ | $(4.139 \pm .429)\times10^{12}$ | $(1.607 \pm .124)\times10^{12}$ | $(3.946 \pm .204)\times10^{11}$ | $(6.562 \pm .351)\times10^{10}$ |
| 8 | $(2.732 \pm .107)\times10^{14}$ | $(1.634 \pm .16)\times10^{14}$ | $(7.394 \pm .872)\times10^{13}$ | $(2.772 \pm .216)\times10^{13}$ | $(7.804 \pm .575)\times10^{12}$ |

Table I (b)



| $\ell$ \ $x_4$ | 0 | 1 | 2 | 3 | 4 |
|---|---|---|---|---|---|
| 1 | $(1.367 \pm .03) \times 10^{3}$ | $(1.073 \pm .049) \times 10^{2}$ | 0.0 | 0.0 | 0.0 |
| 2 | $(4.809 \pm .148) \times 10^{4}$ | $(5.352 \pm .177) \times 10^{3}$ | $(6.637 \pm .454) \times 10^{1}$ | 0.0 | 0.0 |
| 3 | $(2.122 \pm .07) \times 10^{6}$ | $(5.779 \pm .197) \times 10^{7}$ | $(3.835 \pm .27) \times 10^{4}$ | $(6.61 \pm .737) \times 10^{2}$ | 0.0 |
| 4 | $(8.268 \pm .4) \times 10^{7}$ | $(3.029 \pm .146) \times 10^{7}$ | $(3.485 \pm .215) \times 10^{6}$ | $(1.037 \pm .081) \times 10^{5}$ | $(7.387 \pm .168) \times 10^{3}$ |
| 5 | $(3.1 \pm .231) \times 10^{9}$ | $(1.454 \pm .093) \times 10^{9}$ | $(3.121 \pm .211) \times 10^{8}$ | $(2.625 \pm .201) \times 10^{7}$ | $(1.262 \pm .13) \times 10^{6}$ |
| 6 | $(1.11 \pm .116) \times 10^{11}$ | $(5.871 \pm .467) \times 10^{10}$ | $(1.844 \pm .145) \times 10^{10}$ | $(2.829 \pm .222) \times 10^{9}$ | $(2.547 \pm .235) \times 10^{8}$ |
| 7 | $(3.76 \pm .47) \times 10^{12}$ | $(2.088 \pm .197) \times 10^{12}$ | $(8.657 \pm .819) \times 10^{11}$ | $(2.351 \pm .192) \times 10^{11}$ | $(4.368 \pm .352) \times 10^{9}$ |
| 8 | $(1.186 \pm .153) \times 10^{14}$ | $(6.761 \pm .734) \times 10^{13}$ | $(3.318 \pm .377) \times 10^{13}$ | $(1.442 \pm .131) \times 10^{13}$ | $(4.548 \pm .371) \times 10^{12}$ |

Table I (a)

| Padé | K = 0.085 | | K = 0.09 | | K = 0.095 | |
|---|---|---|---|---|---|---|
| | $am_{J/\psi}$ | $f^{-1}_{J/\psi}$ | $am_{J/\psi}$ | $f^{-1}_{J/\psi}$ | $am_{J/\psi}$ | $f^{-1}_{J/\psi}$ |
| 1/1 | 3.13 | .0783 | 2.97 | .0958 | 2.78 | 0.119 |
| 2/1 | 3.27 | .0744 | 3.15 | .0891 | 3.03 | 0.107 |
| 3/1 | 3.25 | .0747 | 3.13 | .0896 | 3.00 | 0.108 |
| 4/1 | 3.26 | .0746 | 3.14 | .0894 | 3.01 | 0.107 |
| 5/1 | 3.26 | .0746 | 3.14 | .0894 | 3.01 | 0.107 |
| 6/1 | 3.26 | .0746 | 3.14 | .0893 | 3.01 | 0.107 |
| 1/2 | 3.25 | .0749 | 3.13 | .0899 | 3.01 | 0.109 |
| 2/2 | 3.25 | .0748 | 3.13 | .0897 | 2.99 | 0.108 |
| 3/2 | 3.22 | .0754 | 3.08 | .0912 | 2.99 | 0.112 |
| 4/2 | 3.26 | .0746 | 3.14 | .0894 | 2.90 | 0.107 |
| 5/2 | 3.26 | .0746 | 3.14 | .0893 | 3.01 | 0.107 |
| 1/3 | 3.25 | .0747 | 3.13 | .0895 | 3.01 | 0.108 |
| 2/3 | 3.26 | .0746 | 3.14 | .0893 | 3.00 | 0.107 |
| 3/3 | 3.26 | .0746 | 3.14 | .0893 | 3.01 | 0.107 |
| 4/3 | 3.26 | .0746 | 3.14 | .0893 | 3.01 | 0.107 |
| 1/4 | 3.26 | .0746 | 3.14 | .0893 | 3.01 | 0.107 |
| 2/4 | 3.26 | .0746 | 3.14 | .0893 | 3.01 | 0.107 |
| 3/4 | 3.26 | .0746 | 3.14 | .0893 | 3.01 | 0.107 |
| 1/5 | 3.26 | .0746 | 3.14 | .0893 | 3.01 | 0.107 |
| 2/5 | 3.26 | .0746 | 3.14 | .0893 | 3.01 | 0.107 |
| 1/6 | 3.26 | .0746 | 3.14 | .0893 | 3.01 | 0.107 |

Table 2



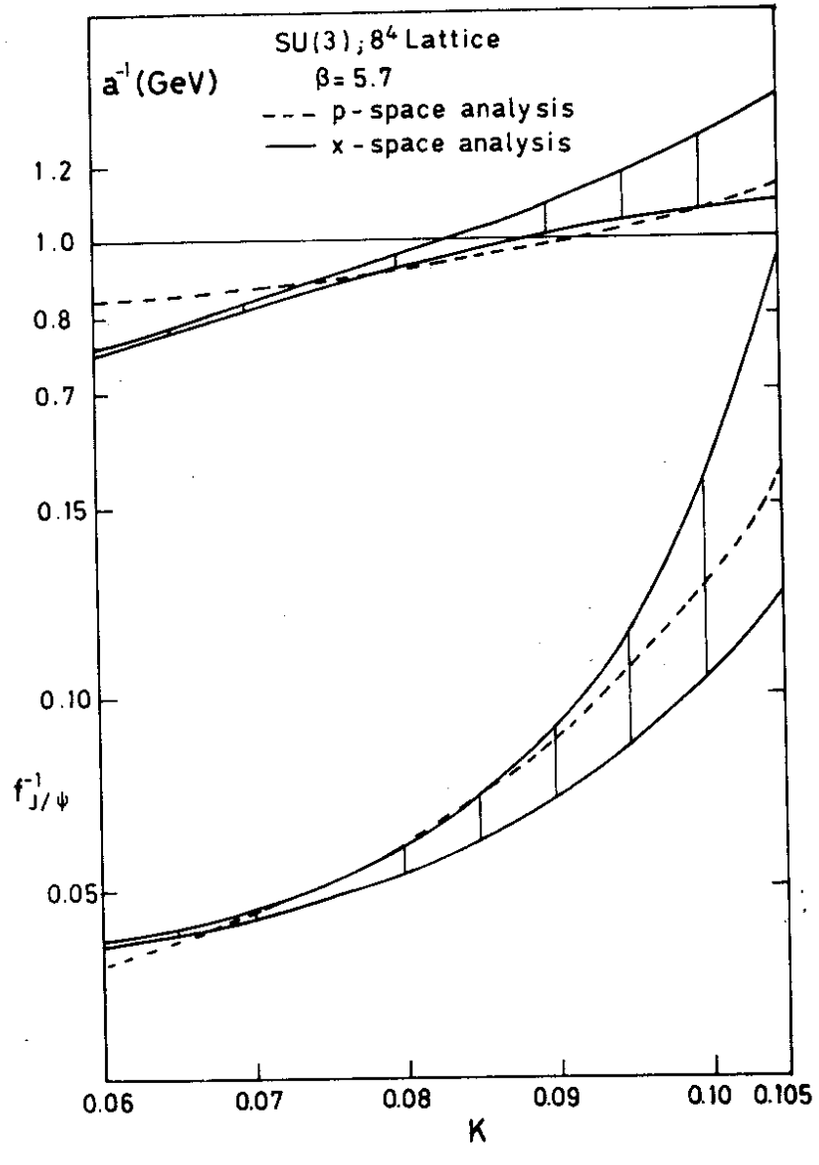


Fig. 1

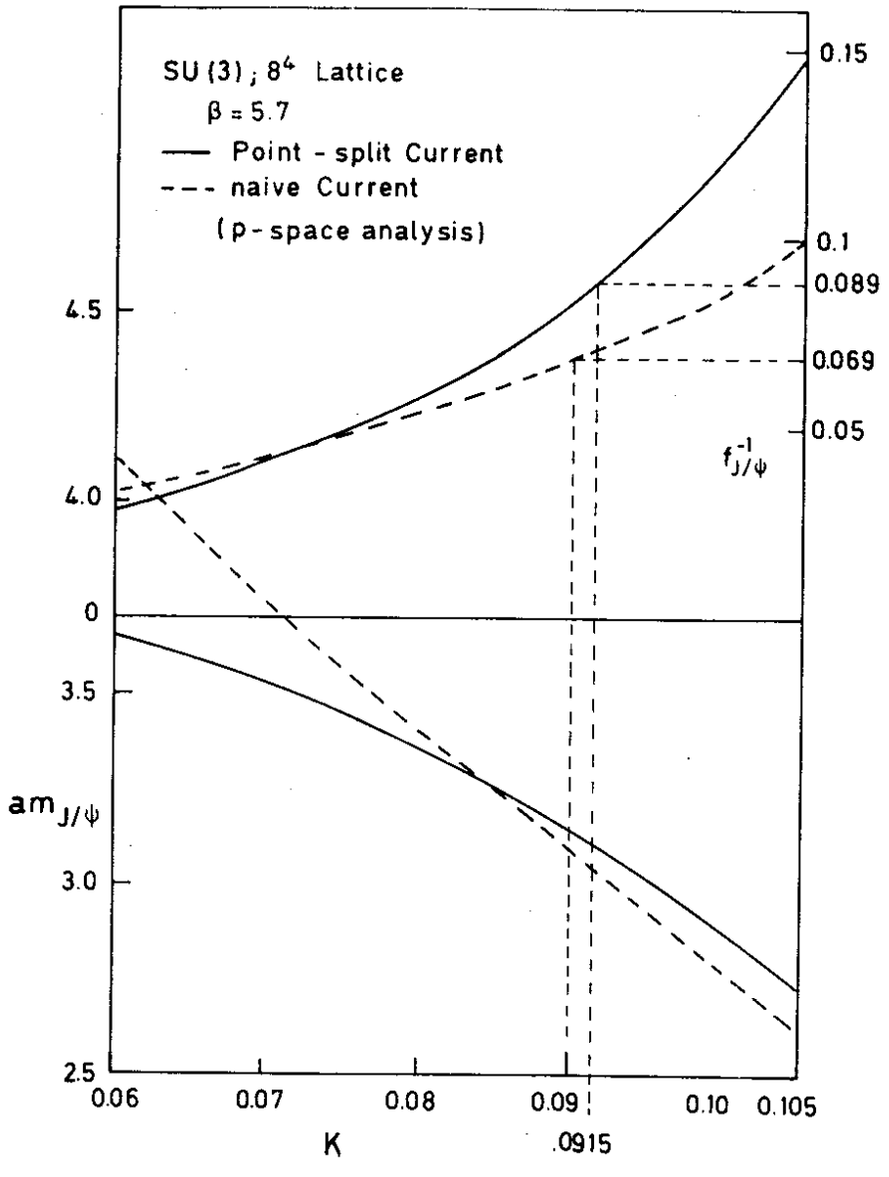
SU(3); $8^4$ Lattice
β = 5.7
Point - split Current
naive Current
(p-space analysis)
0.15
0.1
0.089
0.069
0.05
$f^{-1}_{J/\psi}$
4.5
4.0
0
3.5
3.0
2.5
$am_{J/\psi}$
0.06
0.07
0.08
0.09
0.10
0.105
K
.0915

Fig. 2